Journal of Alloys and Compounds 671 (2016) 184–191

Contents lists available at ScienceDirect

Journal of Alloys and Compounds

journal homepage: http://www.elsevier.com/locate/jalcom

The effect of structural ordering on the magnetic, electronic, and optical properties of the $LaPbMnSbO_6$ double perovskite

V.S. Zhandun [a, b, *], V.I. Zinenko [a]

[a] Kirensky Institute of Physics, Russian Academy of Sciences, Siberian Branch, Akademgorodok 50, bld. 38, Krasnoyarsk, 660036 Russia
[b] Reshetnev Siberian State Aerospace University, Krasnoyarskiy Rabochii 31, Krasnoyarsk, 660037, Russia

ARTICLE INFO

Article history:
Received 21 October 2015
Received in revised form
6 February 2016
Accepted 9 February 2016
Available online 12 February 2016

Keywords:
Ab initio calculation
Double perovskite
Magnetic materials
Optical properties
Electronic properties
Magnetic properties
Layer compound

ABSTRACT

The interplay between the magnetic, electronic, and optical properties and the cation structural ordering in the $LaPbMnSbO_6$ double perovskite is studied using the Vienna Ab Initio Simulation Package (VASP). The layer and rock-salt cation ordering types are investigated. Both of them are of great importance. The rock-salt ordering of B-site cations is one of the most frequently met cation ordering types in double perovskites; the layer ordering of both cations, which can be considered as a heterostructure, is interesting for fundamental research and experimental synthesis. It was established that the properties of the two investigated structures are strongly different. The compound with the layered structure exhibits the behavior typical of a semimetal with the ferromagnetic configuration of magnetic moments, which is unusual for a double perovskite. The rock-salt structure behaves as an antiferromagnetic insulator. Another surprising feature of the structure with the layer ordering is the coexistence of a polar phase and the metal-type conductivity. The calculated optical characteristics of the two ordered structures are compared with the experimental dates.

1. Introduction

In recent years, the development of novel crystal- and film-growth technology has evoked a keen interest in new materials with the magnetic, optical, and other properties promising for application, including the perovskite-like compounds, such as $AA'BB'O_6$ double perovskites intensively studied in the last decade [1–10]. The $AA'BB'O_6$ compounds containing rare-earth or transition metal magnetic ions attract special attention of researchers [6–10]. The coexistence of the ferroelectric and magnetic properties makes these compounds possible candidates for application in modern electronic devices as magnetoelectrics. The variety of the crystal structures with the monoclinic, orthorhombic, tetragonal, and trigonal symmetry intrinsic to this class of compounds gives rise to the diverse ferroelectric, magnetic, optical, piezoelectric, and magnetoelectric properties. The unique characteristics of these materials originate from their chemical composition and the type and degree of cation structural ordering. The most fully studied ordering type is the rock-salt ordering of B and B′ cations [11]. However, the simultaneous ordering of A, A′ and B, B′ cations with four different ions can lead to the new useful properties [12]. In addition, the simultaneous layer ordering of A- and B-site cations is interesting for searching for new heterostructures that can be used in modern technology.

The Sb-based oxides are still unstudied; however, according to the available literature data, these compounds exhibit the intriguing properties. Retuerto et al. [13] reported the existence of the singular ferromagnetism in the ordered Ca_2CrSbO_6 compound, where the magnetic coupling path is separated by nonmagnetic Sb^{5+} ions. In Refs. [14,15], it was shown that the competing magnetic interactions in the Sb-based double perovskites lead to the extraordinary magnetic properties. In Refs. [1,2], the $LaPbMeSbO_6$ double perovskites with magnetic ions (Me = Mn, Fe, Co, or Ni) were synthesized and investigated. In the synthesized compounds, A-site cations were disordered and B-site cations were ordered in the rock-salt structure. The low-symmetry ground state is nonpolar (sp. gr. $P2_1/n$). It was established that all the synthesized compounds are antiferromagnetic insulators with Neel temperatures of about 10 K. However, the effect of simultaneous ordering of A and B cations on the electronic, magnetic, optical, and polar properties of the Sb-based compounds still remains unclear.

In Refs. [16], using the ab initio methods, we studied the

* Corresponding author. Kirensky Institute of Physics, Russian Academy of Sciences, Siberian Branch, Akademgorodok 50, bld. 38, Krasnoyarsk, 660036 Russia.
E-mail address: jvc@iph.krasn.ru (V.S. Zhandun).

http://dx.doi.org/10.1016/j.jallcom.2016.02.085
0925-8388/

hypothetical ordered structure of these perovskites with the preferred layer ordering of A-site cations and the rock-salt ordering of B-site cations. We showed that this type of cation ordering results in the occurrence of ferroelectric polarization in the low-symmetry polar phase, along with the antiferromagnetic ordering of magnetic moments; i.e., the compound acquires the magnetoelectric properties. Thus, the ab initio calculation makes it possible to predict the properties of hypothetical ordered compounds, which can differ from those of the disorder compounds.

Here, we report the results of the ab initio calculation of the structural, magnetic, electronic, and optical properties of the ordered $LaPbMnSbO_6$ double perovskite with a magnetic ion in two structural configurations corresponding to different cation ordering types, i.e., the layer and rock-salt ordering of both types of cations.

In Section 2, we describe in detail the ab initio calculation. Section 3.1 is devoted to the calculation of the structural properties and lattice dynamics. The calculated electronic and magnetic properties of the $LaPbMnSbO_6$ double perovskite in different structural modifications are described in Section 3.2. Section 3.3 is devoted to the calculation of the optical properties. In Section 3.4, we discuss the results obtained and provide explanations. To sum up, we make the conclusions.

2. Calculation method

The calculations were performed using the Vienna Ab Initio Simulation Package (VASP) with Projector-Augmented Waves pseudopotentials. The exchange-correlation functional was chosen within the Perdew–Burke–Ernserhoff parameterization and generalized gradient approximation [17,18]. The valence electron configuration of the Mn magnetic ion was $3p^6 4s^2 4d^5$. We used the GGA + U method within the Dudarev approximation [19], where $U' = U - J$ was assumed to be $U' = 5$ eV for d electrons of the Mn ion. All the calculations were spin-polarized. The Brillouin-zone integration was performed on the $6 \times 6 \times 4$ Monkhorst–Pack grid [20] using the tetrahedron technique. The plane-wave cutoff energy was 500 eV. The lattice parameters and atomic coordinates were optimized until the forces acting on the atoms became less than 0.02 eV.

3. Results and discussion

3.1. The structural properties

As is known [11,21], there are three types of cation ordering on the A- or B-sites of the $AA'BB'O_6$ double perovskite. The most widely spread type is the cation ordering in the rock-salt (R) structure along the [111] direction of the perovskite unit cell. In addition, the cations can be ordered along the [001] direction; in this case, the so-called layer ordering (L) is implemented. The rarest type is the columnar (C) ordering, when the cations are ordered along the [110] direction.

The simultaneous ordering of A- and B-site cations yields nine possible types of the ordered structures [11,21]. Here, we investigate two of them, specifically, the simultaneous ordering of A and B cations in the rock-salt structure (RR) and the simultaneous layer ordering of both types of cations (LL). It should be noted that the second variant is quiet rarely met (see examples of compounds with this ordering type in Ref. [11]), but it can be considered as heterostructure.

The high-symmetry phases of the ordered structures under study are shown in Fig. 1. We used the $\sqrt{2}a \times \sqrt{2}a \times 2a$ double supercell (a is the lattice parameter of the perovskite structure) consisting of 20 atoms, where the in-plane axis of a new cell was assumed to be parallel to the face diagonals of the perovskite cell.

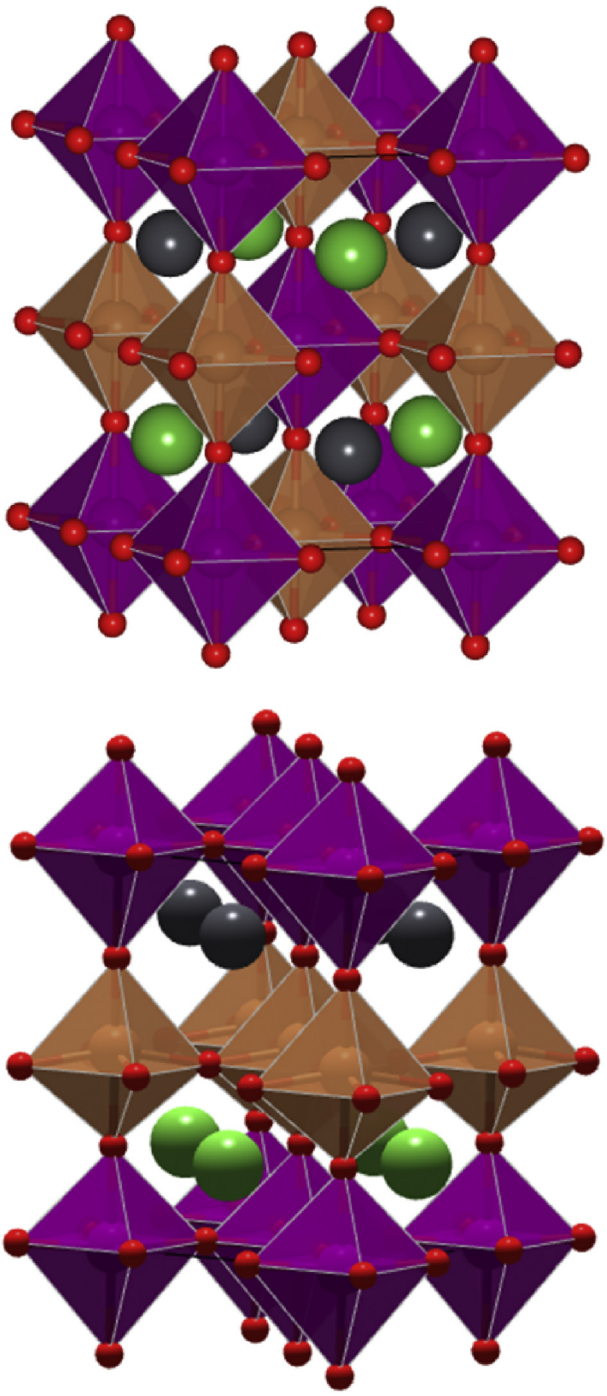

Fig. 1. Structures of the $LaPbMnSbO_6$ double perovskite with the RR (top panel) and LL ordering (bottom panel) of cations. Dark and green balls show Pb and La atoms, respectively. SbO_6 oxygen octahedra are colored with orange and MnO_6 oxygen octahedra, with purple. (For interpretation of the references to colour in this figure legend, the reader is referred to the web version of this article.)

The parameters of the structures were fully optimized for the ferromagnetic (F) and antiferromagnetic (AF) magnetic configurations. The optimized lattice parameters are given in Table 1.

The main result of the optimization of atomic positions in the lattice is the shift of oxygen ions toward Sb atoms. In the structure with the RR cation ordering, the Sb–O distance is 1.98 Å and the Mn–O distance is 2.11 Å. In the structure with the LL ordering, these

Table 1
Lattice parameters (Å) for different types of the structural and magnetic ordering.

	RR	LL
AF	a = 5.78, c = 8.17	a = 5.76, c = 8.36
F	a = 5.78, c = 8.18	a = 5.74, c = 8.41

distances are 2.05 Å and 2.15 Å, respectively.

The calculation of the lattice dynamics disclosed the structural instability of the high-symmetry phases of the compound in the both structural modifications, including unstable polar modes (the unstable vibrational modes at the center of the Brillouin zone are given in Table 2).

To find the stable low-symmetry structures, the most unstable modes were frozen and the structures were fully relaxed. (The symmetry of unstable vibrational modes of the double perovskite with different types of cation ordering and the low-symmetry structures were thoroughly analyzed in Refs. [12]; the results of analysis agree well with the data reported here). The obtained stable low-symmetry structures have polar symmetry groups *R3* for the RR cation ordering and *Pa* for the LL one.

Structural distortions in the low-symmetry phase are related mainly to displacements of Pb and La cations and to minor rotation and tilt of oxygen octahedra. Further calculations showed the insignificant difference between the behavior of the electronic, magnetic, and optical properties of the high- and low-symmetry phases. Therefore, below we consider only the properties of the high-symmetry phase.

3.2. Electronic and magnetic properties of the high-symmetry phase

The magnetic and electronic properties of the compound with both ordering types were calculated within the GGA + U approximation for the F and AF magnetic configurations. The obtained structure energies and magnetic moments are given in Table 3. In the structure with the RR cation ordering, the AF configuration of the magnetic moments is preferred, in which the magnetic moments of Mn atoms in different planes are oppositely directed. This is consistent with the experimental data reported in Refs. [1,2], where the B-site magnetic cations were also ordered in the rock-salt structure. In the structure with the layer ordering of both A- and B-site cations, the ferromagnetic ordering is preferred.

Fig. 2 illustrates the comparison of the band structures and densities of electronic states (DOS) of the investigated structures. In the both structures, the main contribution to the occupancy of the states below the Fermi level is made by *d*-electrons of manganese (both t_{2g} and e_g) and *p*-electrons of oxygen, which leads to the strong hybridization between the *d*- and *p*-orbitals of manganese and oxygen, respectively. This hybridization near the Fermi level attracts attention as a cause of polar distortions in the both structures. It should be noted that all majority spin *d*-states of Mn are occupied, whereas all minority spin *d*-states are empty, which ensures the high-spin state of Mn atoms.

Table 2
Calculated vibration frequencies of unstable modes (mode symmetry is given in parentheses).

ω, cm^{-1}	
RR	LL
220i (A_{1u})	218i (A_{1u})
219i (E_g)	143i (E_g)
147i (A_{1u})	111i (A_{1u})
136i (E_u)	75i (E_u)
132i (E_g)	57i (E_g)

Table 3
Energies E of the ordered structures and magnetic moments μ for different types of the structural and magnetic ordering.

	RR		LL	
	E, eV	μ, μ_b	E, eV	μ, μ_b
AF	−137.184	4.62	−136.619	4.55
F	−137.137	4.64	−136.832	4.48

The RR-ordered structure of the $LaPbMnSbO_6$ compound (top panel in Fig. 2) exhibits the nonmetal behavior with an energy gap of 1.4 eV, which is typical of the double perovskites [21]. Surprisingly, the compound with the LL-ordered cations (middle and bottom panels in Fig. 2) behaves similarly to a semimetal with the gap about 2 eV in the minority spin DOS (bottom panel in Fig. 2). Meanwhile, the majority spin DOS (middle panel in Fig. 2) has a peak at the Fermi level, which is related to t_{2g} electrons of manganese and *p* electrons of oxygen. This causes the appearance of the spin polarization at the Fermi level (~80%) (inset to Fig. 2), which can be interesting for spintronic applications.

Thus, the change in the ordering type of magnetic B-site cations from the rock-salt to layer one leads to the extraordinary electronic and magnetic properties of the double perovskite under study. In Section 3.4, we try to explain this phenomenon.

We should to notice one more interesting feature of the compound with LL cation ordering. Fig. 3 shows the peculiarities of the majority spin state band structure near the Fermi level in the *GX*, *MG*, *ZR*, and *AZ* directions of the Brillouin zone of the compound with the LL cation ordering (Fig. 3). Two adjacent bands above the Fermi level have the maxima and minima at the same point of the Brillouin zone. The lower band is filled with t_{2g} electrons of manganese and *p* electrons of oxygen; the upper band has the empty e_g states of manganese and *p* states of oxygen. It can be seen that these bands are almost intersect at the above-mentioned points of the Brillouin zone. Moreover, the sharp band shape at these points is indicative of the linear law of dispersion of the electron energy. There are four such nodes in the band structure, which are distant from one another by a half of the reciprocal lattice vector in the *k* space. Although the features are localized above the Fermi level by 0.5 eV, this behavior of the bands is very similar to the behavior of the so-called Weyl semimetals [22,23] observed, in particular, in double perovskites [24]. However, this item requires further investigations.

3.3. Optical properties

The optical properties of a substance can be described by the dispersion dependence of permittivity $\varepsilon(\omega)$. The knowledge of real (ε') and imaginary (ε'') parts of the permittivity makes it possible to establish the optical characteristics, including refractive index *n*, extinction coefficient *k*, loss function *L*, absorption coefficient α, and reflectance *R*. The real and imaginary parts of the permittivity were determined using the ab initio calculations; the other optical characteristics were determined using the permittivity value as

$$n = \sqrt{\frac{|\varepsilon| + \varepsilon'}{2}} \quad (1)$$

$$k = \sqrt{\frac{|\varepsilon| - \varepsilon'}{2}} \quad (2)$$

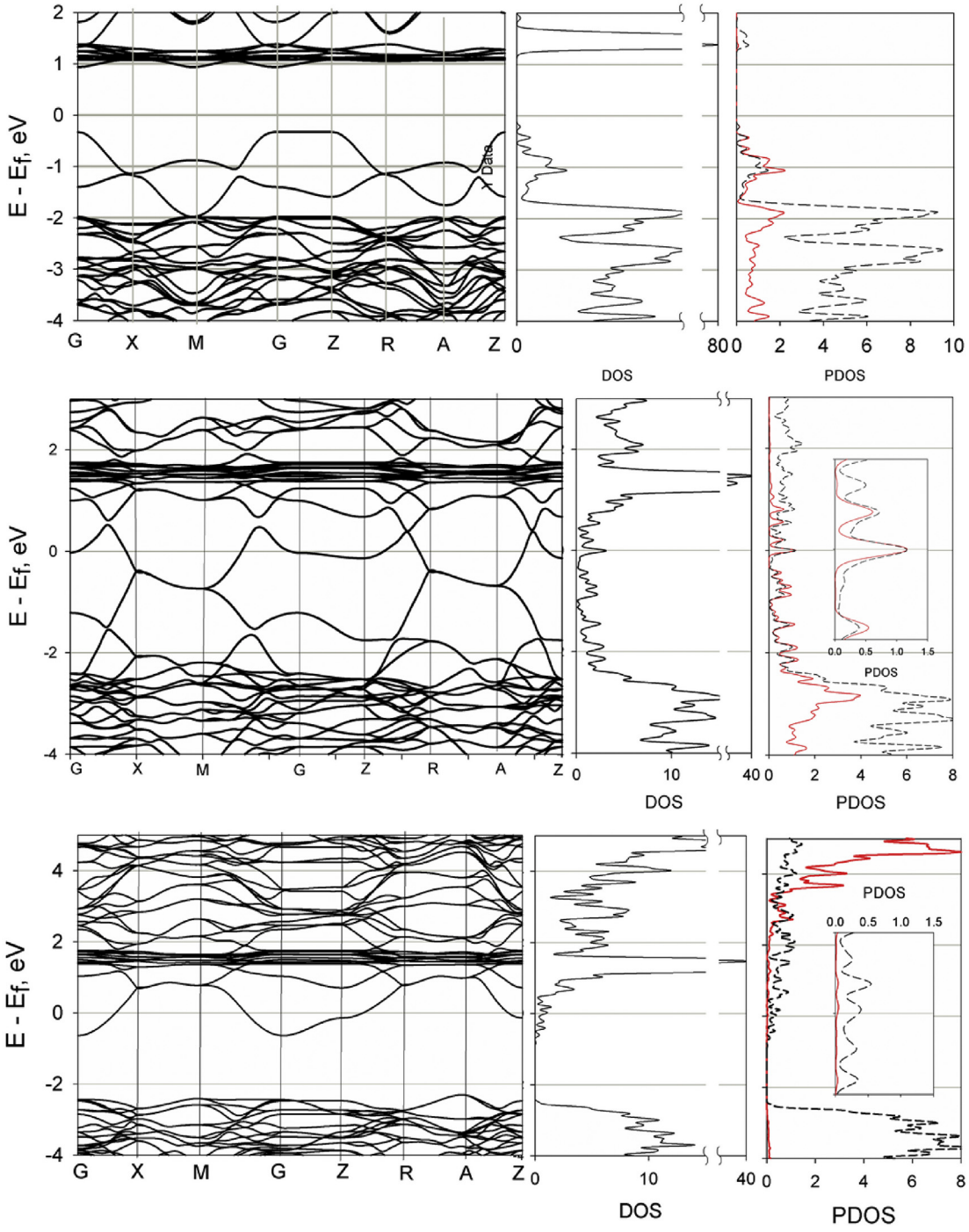

Fig. 2. Top panel: band structure and full and partial densities of electronic states (DOS) for AF $LaPbMnSbO_6$ with the RR cation ordering. Middle panel: the same for the majority spin state of ferromagnetic $LaPbMnSbO_6$ with the LL cation ordering. Bottom panel: the same for the minority spin state of ferromagnetic $LaPbMnSbO_6$ with the LL cation ordering. Inset in the middle and bottom panels: DOS near the Fermi level. Manganese *d* states (red line) and oxygen *p* states (dashed line). The energy zero coincides with the Fermi energy. (For interpretation of the references to colour in this figure legend, the reader is referred to the web version of this article.)

$$R = \frac{(n-1)^2 + k^2}{(n+1)^2 + k^2} \quad (3)$$

$$L = \frac{\varepsilon''}{|\varepsilon|} \quad (4)$$

$$\alpha = \frac{2wk}{c} \quad (5)$$

The results of the calculation are presented in Figs. 4 and 5. The obtained curves have pronounced features, since we did not use the phenomenological smoothing of the theoretical curves, hoping that further experiments, including the low-temperature ones, will help establishing a more detailed structure. It can be seen that the

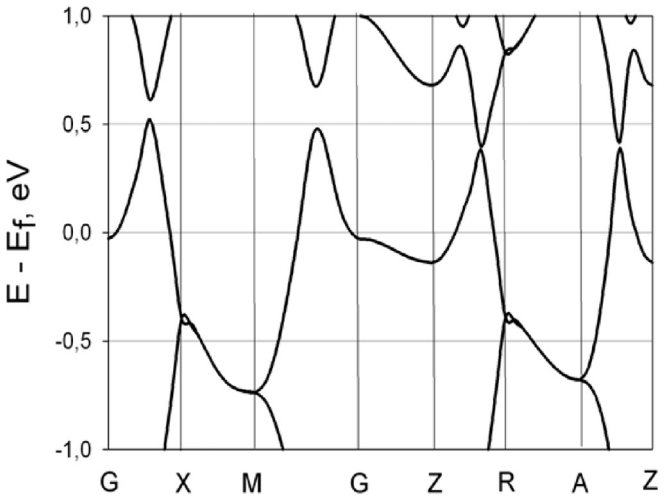

Fig. 3. Band structure of the majority spin state of $LaPbMnSbO_6$ with the LL cation ordering near the Fermi energy. The energy zero coincides with the Fermi energy.

optical properties at the two considered structural ordering types are also different. In the RR-ordered compound, the intraband transition does not occur, while in the LL-ordered compound we observed the free-electron-like behavior at low energies (the Drude plasma frequency related to the intraband transition is 4.1 eV). The presence of conduction electrons causes the features in the optical characteristics of the LL-ordered structure in the low-energy range.

For the both structures, the imaginary part of the permittivity has two pronounced resonance peaks corresponding to the resonance line in its real part. The highest peak is located at an energy of about 5 eV and related to the electron interband transitions from the mixed *p-d* bands at energies from −2 to −5 eV (Fig. 2) to the empty states above the Fermi level. The other peak with the lower intensity is located at about 20 eV. We attribute the resonance at the energy of −18 eV to the interband transition of low-energy lanthanum *s* and *p* electrons.

The energy loss function (top panel in Fig. 5) for the both structures has several peaks: at about 7, 11, and 20 eV for the RR-ordered compound and at about 15 and 22 eV for the LL-ordered one. According to the definition of the loss energy function (4), it

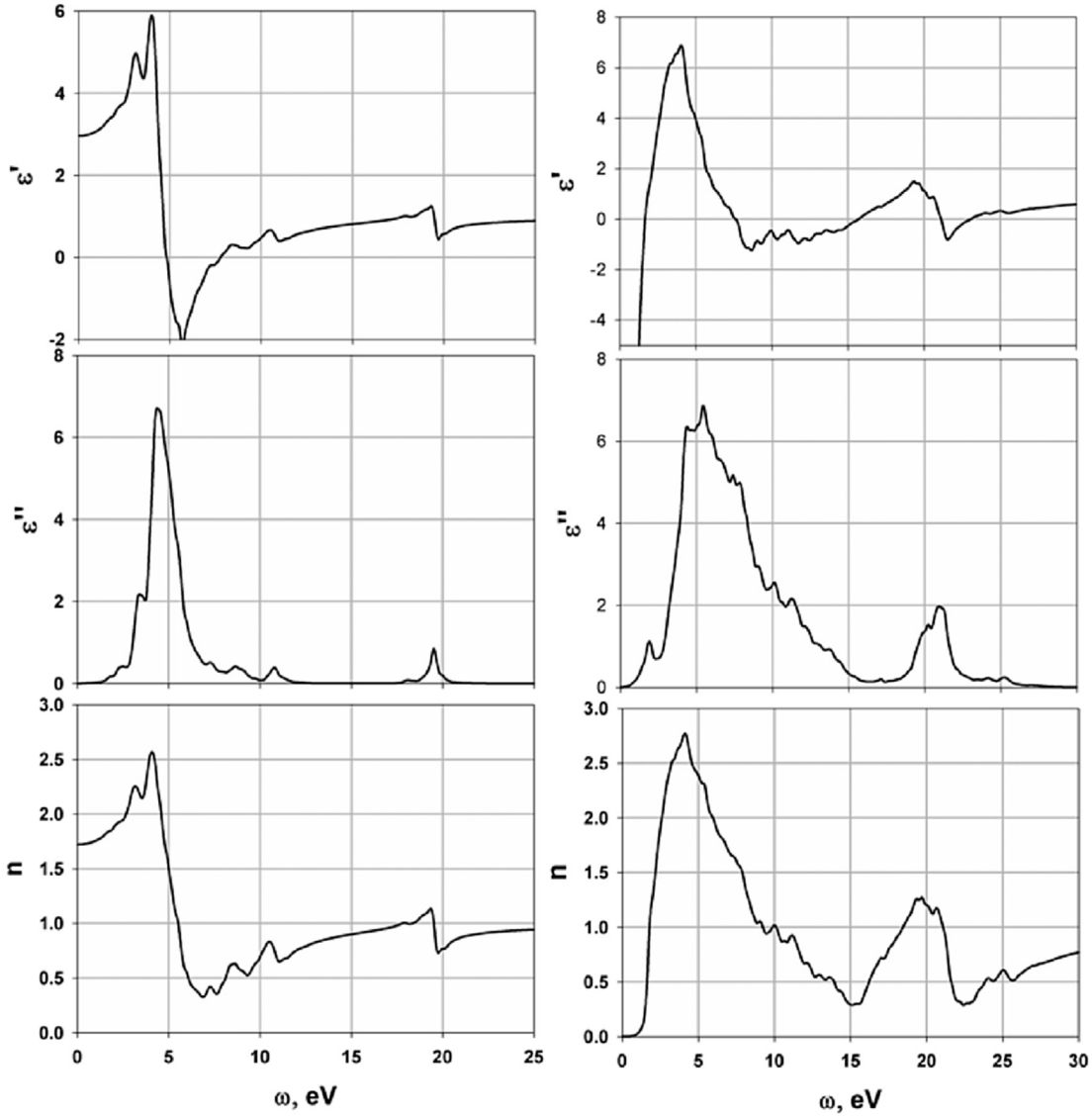

Fig. 4. Real (ε') and imaginary (ε'') parts of the permittivity and refractive index n of $LaPbMnSbO_6$ with the RR- (on the left) and LL (on the right) cation ordering.

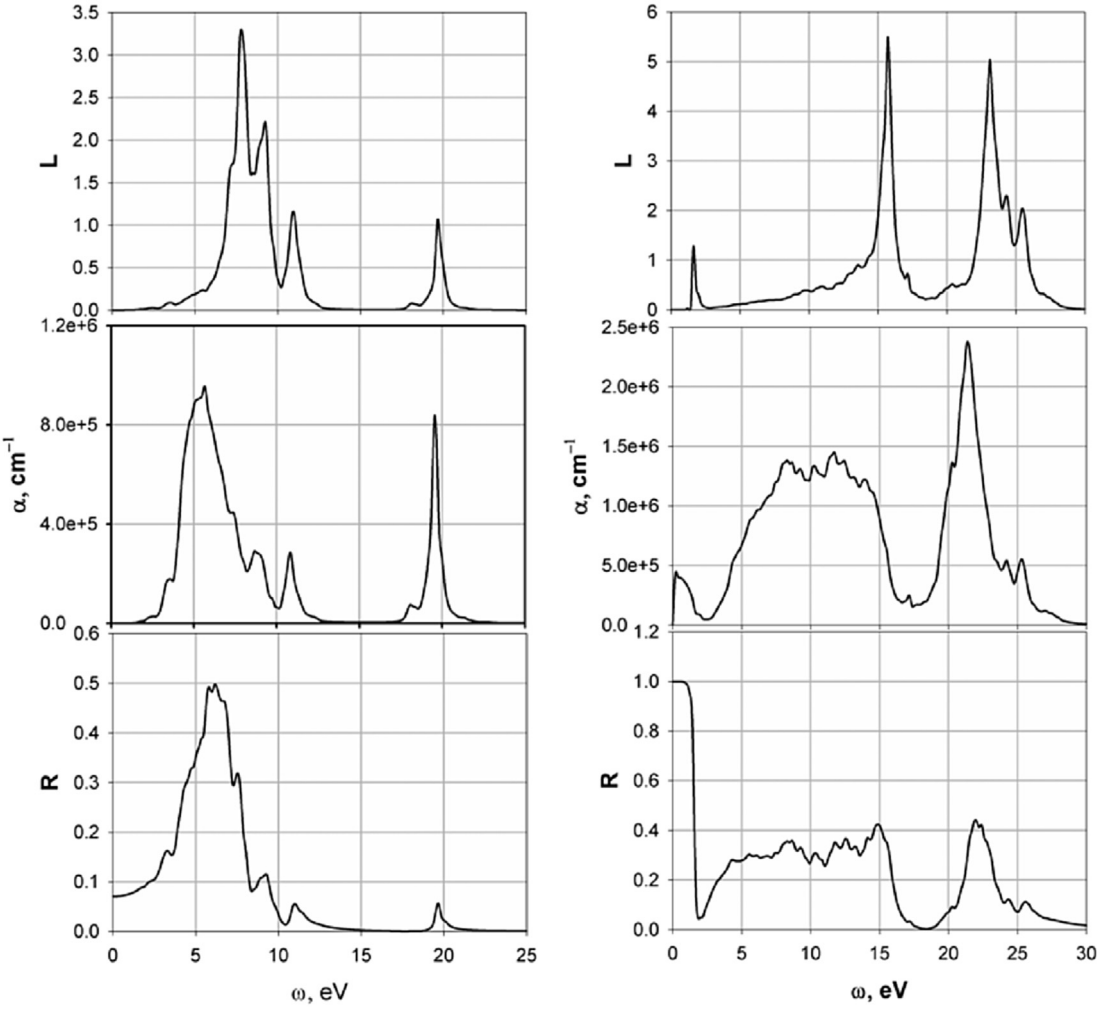

Fig. 5. Loss function L, absorption coefficient α, and reflectance R of $LaPbMnSbO_6$ with the RR (left column) and LL (right column) cation ordering.

is large when ε' is zero and ε'' is small; this regime corresponds to the collective plasma oscillations at high photon energies. In this case, the peaks of the energy loss function of the LL-ordered structure have similar values due to the features of the permittivity dispersion (compare dispersions of the real and imaginary parts of the permittivity on the right panel in Fig. 4).

The wider absorption range of the LL-ordered structure as compared with the absorption range of the RR-ordered structure is also caused by the feature of the band structure. In the LL-ordered structure, the occupied states lie in the wide energy range from −2 to −15 eV, whereas in the RR-ordered structure they lie in the range from −2 to −10 eV (not shown in Fig. 2). Note that, due to the sufficiently large absorption in this range caused by the intense interband transitions, the reflectance of the LL-ordered double perovskite in the middle energy range (bottom panel in Fig. 5) is low.

3.4. Discussion

In this study, we obtained some intriguing results. First, the lattice dynamics calculation reveals the existence of the polar phase in the semimetal $LaPbMnSbO_6$ double perovskite with the LL cation ordering (Section 3.1). The presence of the polar phase in a semimetal could be surprising; meanwhile, it was convincingly confirmed both theoretically and experimentally in recent works [25–27] devoted to the ferroelectric distortions in the $LiOsO_3$ metal compound. The authors of [25,26] discussed the role played by the displacements of A-site cations in establishing the ferroelectric instability in a metal and suggested that the short-range interactions make the crucial contribution to ferroelectricity of the metal. The results obtained by us also show that the displacements of A-site cations play a key role in the polar phase structure distortions.

Second, it was found that the electronic and magnetic properties of the $LaPbMnSbO_6$ double perovskite with different types of the cation ordering are drastically different. We attempted to explain this difference. Figs. 6 and 7 show the electron localization function (ELF) [28] for different atomic planes in the RR- and LL-ordered structures. This function can lie in the range from 0 to 1, where 0 corresponds to the uniform electronic gas and 1, to localized electrons.

It can be seen in Figs. 6 and 7 that electrons of the Sb–O bond are strongly localized; i.e., this bond is covalent. The bond between Mn and O atoms is much weaker. As was mentioned above, the Sb–O and Mn–O distances in the LL structure are larger than in the RR structure, which also leads to the weakening of the interaction between Mn and O atoms in this structure as compared with RR structure. The weakness of the bond between manganese and oxygen atoms in the structure with the LL cation ordering leads to the formation of the nearly uniform electron gas in the plane with Mn

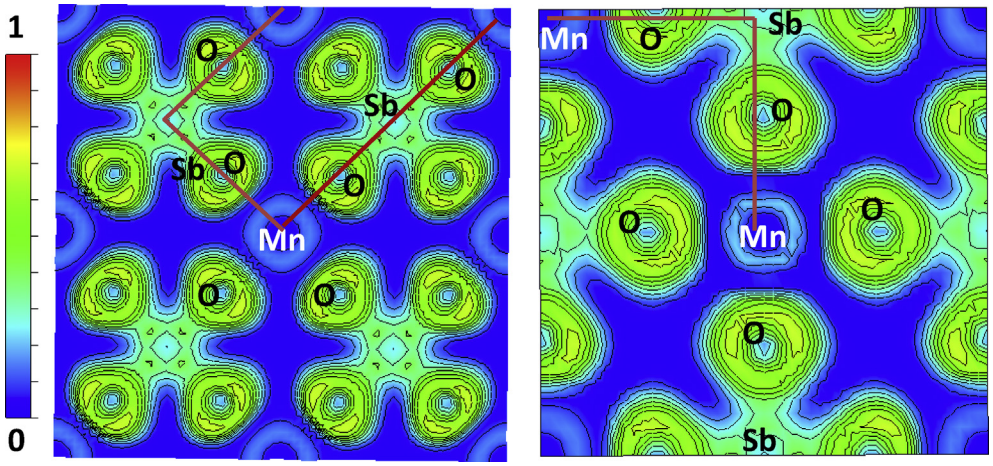

Fig. 6. Electron localization functions for the RR-type ordering. Left panel: the bottom face of the unit cell. Right panel: the (101) plane.

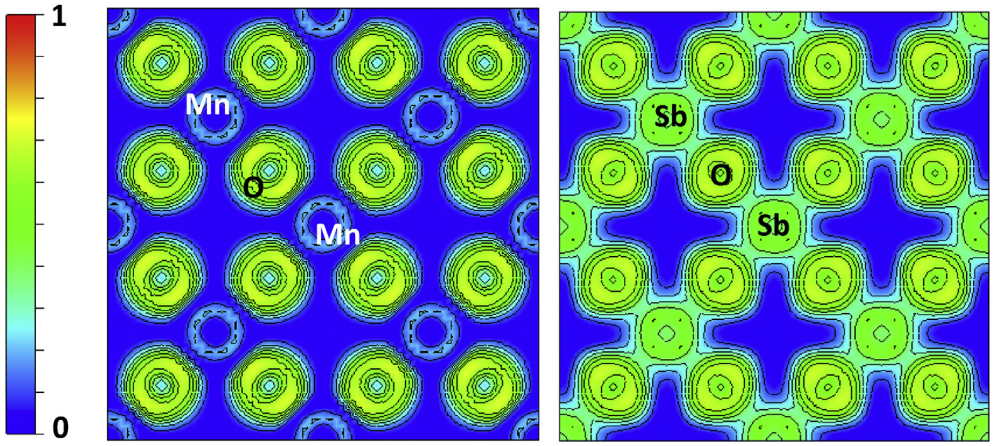

Fig. 7. Electron localization functions for the LL-type ordering (plane (001)). Left panel: the bottom face of the unit cell. Right panel: the plane at the center of the unit cell.

atoms (left panel in Fig. 7) and, thus, to the two-dimensional metal-type conductivity.

To qualitatively explain the dependence of the magnetic state on the cation structural ordering, let us consider the exchange path between magnetic ions. Note that in such a complex compound, the exchange paths can be different and compete with each other. However, we limit the consideration to the near exchange paths between Mn ions. In the structure with the RR cation ordering, the interaction between Mn atoms is implemented via the Mn–O–Sb–O–Mn path (the so-called supersuperexchange, red lines in Fig. 6), which is responsible for the AF ordering in accordance with the Goodenough–Kanamori rules [29]. The ferromagnetism in the LL structure can be understood through the *s–d* exchange model [30]. In the accordance with this model the exchange between magnetic ions in metals can be implemented by conduction electrons (as can be seen from the left panel of Fig. 7 Mn ions are within the region of uniform electron gas). This assumption is supported also by the presence of the electrons with a specified spin direction at the Fermi level (middle panel in Fig. 2), which facilitate the FM alignment of the Mn magnetic moments in the LL ordered structure.

4. Conclusions

The ab initio calculations of the magnetic, electronic, and optical properties of the hypothetical ordered $LaPbMnSbO_6$ double perovskite were performed in the framework of density functional theory using the VASP code. We studied two structural configurations with the simultaneous ordering of A- and B-site cations: layer ordering and rock-salt ordering. The first ordering type attracts attention due to the presence of the layered structure, which can be considered as a heterostructure. We observed the astonishing feature, specifically, the variation in the magnetic and electronic properties, depending on the cation ordering type. The structure with the simultaneous layer ordering of both cations exhibits the semimetal behavior along with the ferromagnetic ordering of magnetic moments, whereas the structure with the RR cation ordering behaves as an AF insulator. The difference in the electronic properties can be explained by different electron charge distribution in the ordered structures. The difference in the magnetic properties possibly originates from different mechanisms of exchange between magnetic ions. Finally, we calculated the optical characteristics of the compounds with both structural types, which can be useful for future experimental investigations.

We demonstrated that the calculated magnetic and electronic properties of the double perovskite with the RR cation ordering agree well with the experimental data reported in Refs. [1,2] and with the results of other studies on the double perovskites with the rock-salt ordering of B-site cations. There is good reason to believe that the ordering of nonmagnetic A-site cations is not crucial for the

magnetic and electronic properties.

The most interesting results were obtained for the LL-ordered double perovskite. First, the metal conductivity (σ_0 = 0.035 MS/m) is unusual for a double perovskite and is observed only at the layer ordering of magnetic cations. This fact, along with the presence of conduction electrons with the significant spin polarization at the Fermi level, is interesting for application, e.g., in spintronics. One more unusual result is the existence of the polar phase in the LL-ordered semimetal double perovskite. In recent time, the existence of the polar phase in metals has been intensively studied, since this phenomenon offers great opportunities for both fundamental research and application, e.g., in creating new material where a ferroelectric soft phonon would stabilize high-temperature superconductivity.

We believe that the obtained results will be useful for fundamental physics and applications, especially if our prognoses will be confirmed in experiments.

Acknowledgments

This work was supported by the Russian Foundation for Basic Research, project no. 15-02-00340-a and the Grant of the President of the Russian Federation for Support of Leading Scientific Schools no. NSH-924.2014.2.

The calculations were performed using computer resources of the National Research Center “Kurchatov Institute” (ui2.computing.kiae.ru). VZ thanks N. Zamkova and I. Sandalov for useful discussions.

References

[1] Y. Bai, L. Han, X. Liu, X. Deng, X. Wu, C. Yao, Q. Liang, J. Meng, J. Meng, J. Solid State Chem. 217 (2014) 64.
[2] D.G. Franco, R.E. Carbonio, G. Nieva, IEEE Trans. Magn. 49 (2013) 4594.
[3] G. Vaitheeswaran, V. Kanchana, A. Delin, Appl. Phys. Lett. 86 (2005) 032513.
[4] D. Stoeffler, C. Etz, J. Phys. Condens. Matter 18 (2006) 11291.
[5] S. Gong, P. Chen, B.G. Liu, JMMM 349 (2014) 74.
[6] D.A. Landínez Téllez, D. Llamosa P, C.E. Deluque Toro, Arles V. Gil Rebaza, J. Roa-Rojas, J. Mol. Struct. 1034 (2013) 233.
[7] D. Serrate, J.M. De Teresa, M.R. Ibarra, J. Phys. Condens. Matter. 19 (2007) 023201.
[8] Y. Fujioka, J. Frantti, M. Kakihana, J. Phys. Chem. B 110 (2006) 777.
[9] Y. Zhang, V. Ji, J. Phys. Chem. Solids 73 (2012) 1116.
[10] Q. Zhanga, G.H. Raoa, Y.G. Xiaoa, H.Z. Dongb, G.Y. Liua, Y. Zhanga, J.K. Lianga, Phys. B 381 (2006) 233–238.
[11] G. King, P.M. Woodward, J. Mater. Chem. 20 (2010) 5785.
[12] N.G. Zamkova, V.S. Zhandun, V.I. Zinenko, Phys.stat.sol. (b) 250 (2013) 1888.
[13] M. Retuerto, M. García-Hernández, M.J. Martínez-Lope, M.T. Fernández-Díaz, J.P. Attfield, J.A. Alonso, J. Mater. Chem. 17 (2007) 3555.
[14] T.K. Mandal, A.M. Abakumov, M.V. Lobanov, M. Croft, V.V. Poltavets, M. Greenblatt, Chem. Mater 20 (2008) 4653.
[15] R. Mathieu, S.A. Ivanov, I.V. Solovyev, G.V. Bazuev, P. Anil Kumar, P. Lazor, P. Nordblad, Phys.Rev. B 87 (2013) 014408.
[16] V.S. Zhandun, V.I. Zinenko, Phys. Solid State 57 (No. 5) (2015) 987.
[17] G. Kresse, J. Furthmuller, Phys. Rev. B 54 (1996) 11169.
[18] J.P. Perdew, K. Burke, M. Ernzerhof, Phys. Rev. Let. 77 (1996) 3865.
[19] S.L. Dudarev, G.A. Botton, S.Y. Savrasov, C.J. Humphreys, A.P. Sutton, Phys. Rev. B 57 (1998) 1505.
[20] H.J. Monkhorst, J.D. Pack, Phys. Rev. B 13 (1976) 5188.
[21] T. Fukushima, A. Stroppa, S. Picozza, J.M. Perez-Mato, Phys. Chem. Chem. Phys. 13 (2011) 12186.
[22] L.X. Yang, Z.K. Liu, Y. Sun, H. Peng, H.F. Yang, T. Zhang, B. Zhou, Y. Zhang, Y.F. Guo, M. Rahn, D. Prabhakaran, Z. Hussain, S.-K. Mo, C. Felser, B. Yan, Y.L. Chen, Nat. Phys. 11 (2015) 728.
[23] Y. Sun, S.-C. Wu, B. Yan, Phys. Rev. B 92 (2015) 115428.
[24] A. Cook, A. Paramekanti, arXiv:1308.3701 V1 [cond-mat.str-el], 16 Aug 2013.
[25] H.J. Xiang, Phys. Rev. B 90 (2014) 094108.
[26] G. Giovannetti, M. Capone, Phys. Rev. B 90 (2014) 195113.
[27] Y. Shi, Y. Guo, X. Wang, A.J. Princep, D. Khalyavin, et al., Nat. Mater. 12 (2013) 1024–1027.
[28] A.D. Becke, K.E. Edgecombe, J. Chem. Phys. 92 (1990) 5397.
[29] a J.B. Goodenough, Phys. Rev. 100 (1955) 564;
b J.B. Goodenough, J. Phys. Chem. Solids 6 (1958) 287;
c J. Kanamori, J. Phys. Chem. Solids 10 (1959) 87.
[30] S.V. Vonsovsky, JETP 16 (1946) 980.